**International Conference on Applied Energy 2019**
**Aug 12-15, 2019, Västerås, Sweden**
**Paper ID: 0934**

# NUMERICAL INVESTIGATION OF HEAT TRANSFER PERFORMANCE OF DEEP BOREHOLE HEAT EXCHANGERS

Yi-fan Sui, Jia-ling Zhu*, Yu-shi Wang, Yu-jiao Lei

Key Laboratory of Efficient Utilization of Low and Medium Grade Energy of Ministry of Education (Tianjin University), Tianjin 300350, China

*Corresponding author: zhujl@tju.edu.cn; Tel: +86-(0)22-27401823; fax: +86-(0)22-27401823.

**ABSTRACT**

The deep borehole heat exchanges (DBHEs) use a coaxial tube to obtain deep geothermal energy, avoiding the problem of groundwater corrosion and recharge, which have great application value. In this paper, a heat transfer model of a DBHE with a depth of 2000m and an outer diameter of 177.8mm is established by Fluent. The effects of various inlet temperature (5~20℃), inlet velocity (0.5~1m/s), thermal conductivity of rock (2.5~3.5W/(m·℃)) and geothermal gradient (0.035~0.045℃/m) on the heat transfer performance in a heating season are studied. The results show that the heat transfer performance of DBHEs decays with time. The rock temperature field is basically invariant outside the radius of 15m. Decreasing the inlet temperature, increasing the inlet velocity, increasing the thermal conductivity of the rock, and increasing the geothermal gradient can increase the heat extraction rate of DBHEs. Under the condition of constant geometric parameters, for every increase of 0.005℃/m in geothermal gradient, the heat extraction rate of the DBHE studied increases by an average of 22.76kW, and for every increase of 0.5W/(m·℃) in the thermal conductivity of the rock, it increases by an average of 26.44kW.

**Keywords:** deep borehole heat exchanger, geothermal energy, numerical simulation, heat transfer

**NONMENCLATURE**

| | |
|---|---|
| *Abbreviations* | |
| DBHE | Deep borehole heat exchanger |
| FVM | Finite volume method |
| *Symbols* | |
| $T$ | Temperature(℃) |
| $t$ | Time(s) |
| $u$ | Velocity(m/s) |
| $S$ | Source term(℃/s) |
| $D$ | Outer diameter(m) |
| $d$ | Inner diameter(m) |
| $A$ | Cross-section area(m$^2$) |
| $\rho$ | Density(kg/m$^3$) |
| $c$ | Specific heat capacity(J/(kg·℃)) |
| $h$ | Heat transfer coefficient(W/m$^2$) |
| $Q$ | Heat extraction rate(kW) |
| $L$ | Depth(m) |
| $\lambda$ | Thermal conductivity(W/(m·℃)) |
| *Subscripts* | |
| f | Fluid |
| if | Inner fluid |
| of | Outer fluid |
| ip | Inner pipe |
| op | Out pipe |
| r | Rock |
| s | Solid |
| i | Inlet |
| o | Outlet |

## 1. INTRODUCTION

Nowadays, the development of renewable energy instead of fossil energy has become a research hotspot. Compared with other renewable energy, geothermal

Selection and peer-review under responsibility of the scientific committee of the 11th Int. Conf. on Applied Energy (ICAE2019).

This work is financially supported by the National Key Research and Development Program of China (Grant No. 2018YFC0604305)

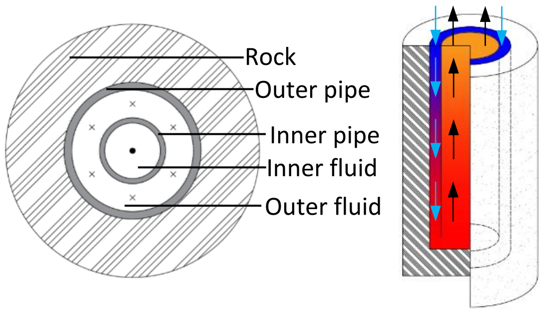


(a)Structure in axial direction (b)Working principle

Fig. 1 Schematic diagram of the DBHE

energy has the advantages of high reserves, safety and stability. According to the depth, geothermal energy can be divided into shallow geothermal energy (0~200m) and deep geothermal energy (≥200m). To better exploit deep geothermal energy, DBHEs are proposed, which is receiving more and more attention.

The working principle of the DBHE is shown in Fig. 1. It has coaxial tube structure, including an inner pipe and an outer pipe, and the outer pipe is in contact with the rock. The working fluid is injected into the outer pipe. It transfers heat with the rock through the outer pipe, and the fluid temperature rises. After reaching the bottom of the coaxial tube, it flows upward into the inner pipe and its temperature deceases because of heat transfer with outer fluid. The working fluid flows in a completely closed cycle, and underground water is not exploited, avoiding problems such as corrosion and scaling of the pipeline and recharge. In addition, the geothermal well of the DBHE has a simple structure and a small floor area, which reduces initial investment and damage to the geological structure.

In recent years, the research on DBHEs has mainly focused on the following three aspects: the key factors affecting the heat transfer performance of coaxial tube, the seasonal heat storage performance of the rock, and the sustainability of DBHEs under a long-term operation condition. In addition, some papers study the application of the DBHE to abandoned oil wells reconstruction or the DBHE system coupled with ground source heat pump.

In this paper, a numerical model of coaxial DBHEs considering the geothermal gradient in rock is established to simulate heat transfer in a heating season through commercial software Fluent. Based on the model established, an analysis is performed to investigate the effects of key factors including inlet velocity, inlet temperature and properties of the rock on the heat transfer performance of DBHEs. Heat extraction rate and outlet temperature are investigated to evaluate the performance. The results of this study can be used for engineering design and optimization of DBHEs.

## 2. MODEL

### *2.1 Physical model*

The geometric model in this study is shown in Fig. 2. Computational domains include working fluid, inner pipe, outer pipe and rock. The main parameters of the DBHE and physical properties of the materials are shown in Table 1.

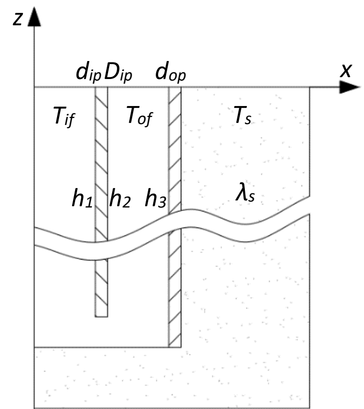


Fig. 2 Geometric model of the DBHE

Table 1 Main parameters of the DBHE

| Parameter | Value |
|---|---|
| Outer pipe(mm) | Ø177.8×9.19 |
| Inner pipe(mm) | Ø110×10 |
| $L_{ip}$(m) | 1998 |
| $L_{op}$(m) | 2000 |
| Working fluid | Water |
| $\lambda_{ip}$(W/(m·℃)) | 0.1 |
| $\lambda_{op}$(W/(m·℃)) | 10 |
| $\rho_{ip}$(kg/m$^3$) | 950 |
| $\rho_{op}$(kg/m$^3$) | 7850 |
| $\rho_r$(kg/m$^3$) | 2650 |
| $c_{ip}$(J/(kg·℃)) | 2300 |
| $c_{op}$(J/(kg·℃)) | 500 |
| $c_r$(J/(kg·℃)) | 1050 |

### *2.2 Model assumption*

The heat transfer process of the DBHE system is composed of the following parts: heat conduction inside the rock and outer pipe, convective heat transfer between the outer fluid and the outer pipe, convective heat transfer between the outer fluid and the inner pipe, heat conduction inside the inner pipe and convective heat transfer between the inner fluid and the inner pipe.

To simplify computation, following assumptions are taken in the model.

- The rock is assumed to be an isotropic uniform continuous solid medium, and pure heat conduction is considered as the only mechanism of heat transfer inside the rock.
- The physical properties of the rock are isotropic, so the heat is not transferred in the tangential direction. The model can be simplified to a 2D axisymmetric model to save computation time.
- The rock is in full contact with the outer pipe wall, and the thermal resistance caused by the gap can be ignored.
- The effect of surface temperature fluctuation on rock temperature is ignored and the surface temperature is regarded as 15℃, annual average temperature of Tianjin.
- The physical parameters of water, inner pipe, outer pipe and rock are constant, which do not change with temperature.

### *2.3 Mesh description*

The computational domain should be semi-infinite. When the boundary of the rock is far enough, its temperature distribution hardly changes with time. Therefore, the computational domain of the rock is selected as a cylindrical space with a radius of 80m and a depth of 2200m.

The equal-scale geometric model of DBHEs is established by ICEM, and meshing is performed to discretize the governing equations by FVM. Structured grids are adopted. The number of total elements of the mesh is 16706.

### *2.4 Mathematical model*

The governing equations mainly include the energy conservation equations of the inner fluid, the outer fluid and the solid.

Heat is transferred from the inner fluid to the inner pipe. The energy conservation equation of the inner fluid is written as Equation 1.

$$\frac{\partial T_{if}}{\partial t} + \frac{\partial u_{if} T_{if}}{\partial z} = \frac{\pi h_1 d_{ip} (T_{w1} - T_{if})}{\rho_f A_{if} c_f} \tag{1}$$

where $h_1$ is the heat transfer coefficient between the inner fluid and the inner wall of the inner pipe, and $T_{w1}$ is the temperature of the inner wall of the inner pipe.

Heat is transferred from the inner pipe and the outer pipe to the outer fluid. The energy conservation equation of the outer fluid is given as Equation 2.

$$\frac{\partial T_{of}}{\partial t} + \frac{\partial u_{of} T_{of}}{\partial z} = S_1 + S_2 \tag{2}$$

$$S_1 = \frac{\pi h_2 D_{ip} (T_{w2} - T_{of})}{\rho_f A_{of} c_f} \tag{3}$$

$$S_2 = \frac{\pi h_3 d_{op} (T_{w3} - T_{of})}{\rho_f A_{of} c_f} \tag{4}$$

where $h_2$ is the heat transfer coefficient between the outer fluid and the outer wall of the inner pipe, $T_{w2}$ is the temperature of the outer wall of the inner pipe, $h_3$ is the heat transfer coefficient between the outer fluid and the inner wall of the outer pipe, and $T_{w3}$ is the temperature of the inner wall of the outer pipe.

The heat transfer inside the solid is pure heat conduction, so heat transfer is represented by the two-dimension heat conduction equation. The energy conservation equation of solids is expressed as Equation 5 for rock, inner pipe and outer pipe.

$$\rho_s c_s \frac{\partial T_s}{\partial t} = \frac{\partial}{\partial z}\left(\lambda_s \frac{\partial T_s}{\partial t}\right) + \frac{1}{x}\frac{\partial}{\partial x}\left(x \lambda_s \frac{\partial T_s}{\partial x}\right) \tag{5}$$

The above governing equations are implemented by setting the Energy Equation and the Viscous Equation in Model of Fluent. The flow is turbulent, so Standard k-epsilon Equation is chosen as Viscous Equation. The convective heat transfer coefficient is calculated by the coupled boundary conditions in Fluent. The governing equations are discretized in the solver by FVM.

To evaluate the heat transfer performance of the DBHE, Heat extraction rate is defined, given as Equation 6 to show heat transferred between the fluid and the rock.

$$Q = \rho_f c_f A_{if} u_{if} (T_o - T_i) \tag{6}$$

### *2.5 Boundary and initial conditions*

According to the previous assumptions, the rock boundary is a constant temperature boundary condition. The heat transfer between the solid and the fluid meets the third boundary condition, expressed by Equation 7. The third boundary condition is achieved by setting the coupled wall boundary condition in Fluent.

$$\hbar (T_w - T_f) = \lambda_s \frac{\partial T_s}{\partial x} \tag{7}$$

The axis *x=0* takes an axis boundary condition. This study does not consider DBHEs coupled with other systems, so the outlet boundary condition is set to outflow. The inlet boundary condition is set to velocity inlet to regulate the temperature and velocity of the inlet fluid.

The initial temperature of the fluid and inner pipe is set to the inlet temperature and the fluid is static. The initial temperature field of the rock is given as Equation 8, with a geothermal gradient, $T_g$.

$$T_r|_{L=z} = 15 + T_g z \tag{8}$$

The model is transient. The time step is set as 900s. The heating season is 135 days long. The Coupled scheme is chosen for calculation.

## 3. RESULTS AND DISCUSSION

### *3.1 Attenuation of heat transfer performance*

Fig. 3 shows the variation of outlet temperature and heat extraction rate with time at different inlet temperatures in a heating season with $u_i$=1m/s, $T_g$=0.035℃/m, and $\lambda_r$=3W/(m·℃).

As can be seen in Fig. 3, both the outlet temperature and the heat extraction rate decrease with time. At an inlet temperature of 10℃, the outlet temperature of the DBHE at the 4th, 8th, 12th, 16th and 20th week is 14.45℃, 14.14℃, 14.03℃, 13.96℃ and 13.91℃, with a reduce percent of 14.5%, 7.2%, 3.5%, 2.3% and 1.7% in last 4 weeks. It can be seen that in the first 8 weeks, the heat transfer performance of DBHEs decreases rapidly. As time goes on, the temperature distribution around the geothermal well tend to be stable.

Since the rock temperature field cannot be restored to the initial temperature field, the heat transfer performance of DBHEs in next heating season will be further attenuated. Therefore, restoring rock thermal storage in the non-heating season is critical to maintaining the heat transfer performance of DBHEs.

### *3.2 Rock temperature distribution*

Fig. 4 shows the rock temperature field at the end of a heating season when $u_i$=1m/s, $T_g$=0.035℃/m, and $\lambda_r$=3W/(m·℃), $T_i$=10℃. It can be seen that the rock temperature distribution surrounding the well varies significantly. The closer to the geothermal well, the more the temperature decreases. Outside the radius of 15 m, the rock temperature barely varies in a heating season. The rock temperature varies greatly in the radial direction, indicating that the rock with simple heat conductivity coefficient cannot effectively restore the heat around the geothermal well, resulting in attenuation of heat transfer performance. The rock temperature distribution can also provide reference for the design of distribution of multiple DBHEs to avoid the heat transfer process interacting with each other.

### *3.3 Effect of inlet conditions*

As shown in Fig. 3, the outlet temperature increases with the increase of the inlet temperature, but the heat extraction rate decreases as the inlet temperature increases. According to the principle of heat transfer, the higher the inlet temperature, the smaller the

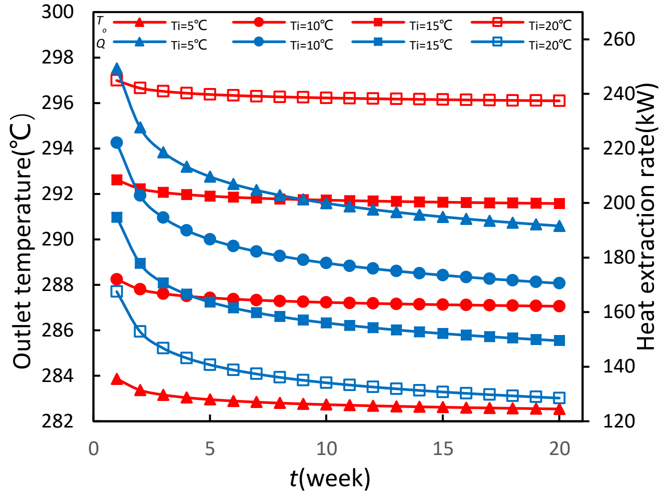


Fig. 3 Variation of outlet temperature and heat extraction rate with time at different inlet temperature

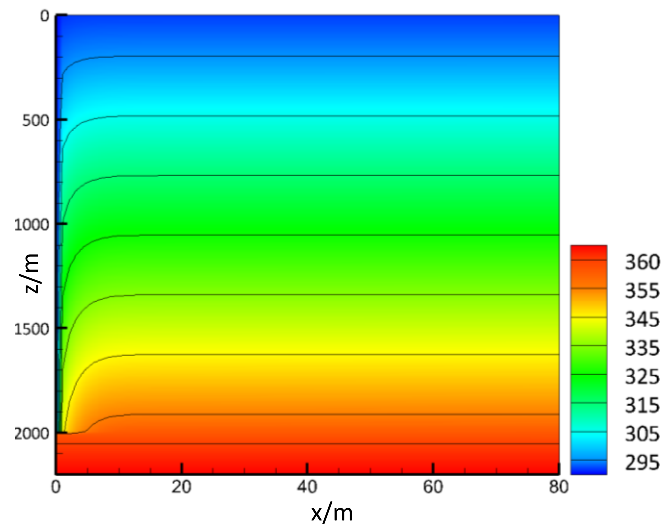


Fig. 4 Rock temperature field at the end of a heating season

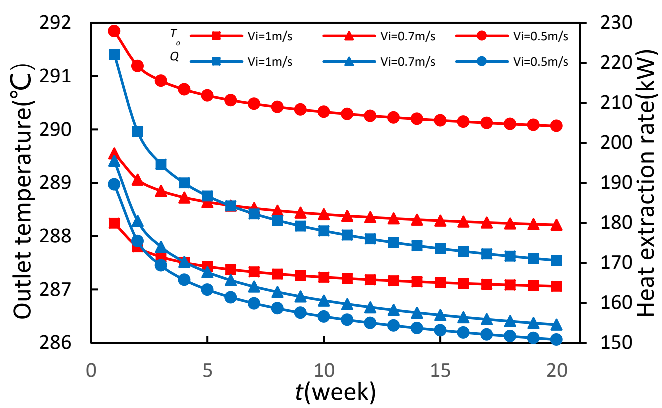


Fig. 5 Variation of outlet temperature and heat extraction rate with time at different inlet velocity

temperature difference between the water and the rock. Although the energy quality is improved, the heat transferred decreases. Compared with 1st week, the heat extraction rates at 5th week at 5℃, 10℃, 15℃, and

20℃ reduce 39.66kW, 35.39kW, 31.11kW, and 26.84kW. The reduce percent is respectively 15.91%, 15.93%, 15.97%, and 16.02%, indicating that as the inlet temperature increases, the attenuation of heat transfer performance increase slowly.

Fig. 5 shows the variation of the outlet temperature and the heating extraction rate with time at different inlet velocity with $T_g$=0.035℃/m, and $\lambda_r$=3W/(m·℃), $T_i$=10℃. It can be seen that as the inlet velocity increases, the outlet temperature of the DBHE decreases and the heat extraction rate increases. When the velocity drops from 1m/s to 0.5m/s, the average temperature difference between the inlet and outlet increases by 75.39%. The increase of the inlet and outlet temperature difference is less than the decrease of the flow rate.

### 3.4 *Effect of rock*

Fig. 6 shows variation of heat extraction rate with time at different the thermal conductivities of the rock when $u_i$=1m/s, $T_g$=0.035℃/m, and $T_i$=10℃. Fig. 7 shows variation of heat extraction rate with time at different geothermal gradient when $u_i$=1m/s, $\lambda_r$=3W/(m·℃), and $T_i$=10℃. It can be seen that as the thermal conductivity of the rock and geothermal gradient increase, the heat extraction rate rises. For every increase of 0.005℃/m in geothermal gradient, the heat extraction rate increases by an average of 22.76kW, and for every increase of 0.5W/(m·℃) in the thermal conductivity of the rock, it increases by an average of 26.44kW.

It can be seen that as the thermal conductivity of the rock increases from 2.5W/(m·℃) to 3.5W/(m·℃), the growth trend of the heat transfer performance of the rock is slowing down. In reality, the thermal conductivity of the rock is in a range of 1.5~3.5W/(m·℃), so increasing thermal conductivity of rock has little significance for improving the heat transfer performance of DBHEs.

### 3.5 *Model validation*

To validate the model, the results of this paper are compared with the results of other papers. Kong summarized some DBHE application case from literature [11]. It can be found that the heat extraction per meter of these cases varies from 43.5W to 188.8W. The depth of these DBHEs varies from 1200m to 2786m. The average heat extraction per meter in this paper varies from 68.48W to 113.63W, which is a reasonable range.

## 4. CONCLUSIONS

In this paper, Fluent is used to establish the model of DBHEs with working fluid of water. The influence of different factors on the heat transfer performance of DBHEs is studied by numerical simulation. The following conclusions are drawn.

(1) The heat transfer performance of DBHEs attenuates with time obviously. Therefore, it is necessary to recover the heat storage of rock in non-heating season to make DBHEs continues to run.

(2) The decrease of inlet temperature and increase of inlet velocity will improve heat transfer performance, but the two methods will reduce energy quality. The actual operation parameters should be in an appropriate range.

(3) Increasing the thermal conductivity of the rock and geothermal gradient will improve heat transfer performance of DBHEs, while the thermal conductivity of the rock has less influence.

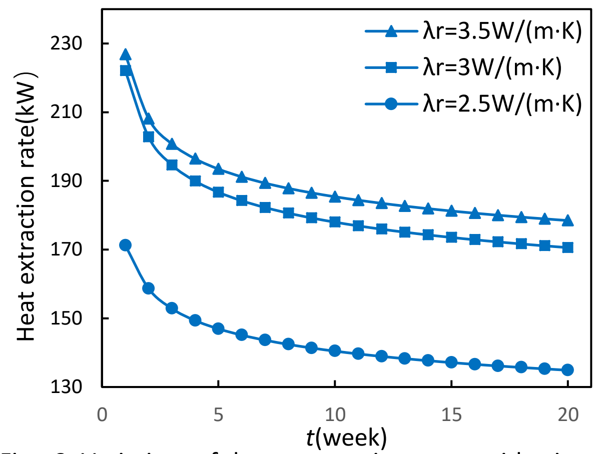


Fig. 6 Variation of heat extraction rate with time at different the thermal conductivity of the rock

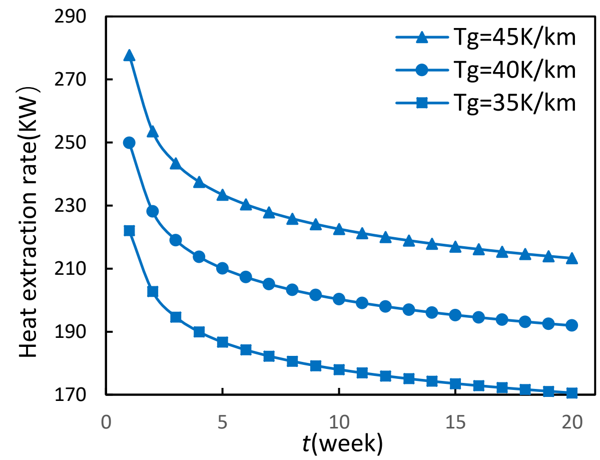


Fig. 7 Variation of heat extraction rate with time at different geothermal gradient

**ACKNOWLEDGEMENT**

The authors gratefully acknowledge the financial support provided by the National Key Research and Development Program of China (Grant No. 2018YFC0604305)

**REFERENCE**

[1] Cai WL, Wang FH, Liu J, et al, and Zhenjun Ma. Experimental and Numerical Investigation of Heat Transfer Performance and Sustainability of Deep Borehole Heat Exchangers Coupled with Ground Source Heat Pump Systems[J]. Applied Thermal Engineering 2019;149:975-86.

[2] Liang F, Diao NR, Shao ZK, et al. A Computationally Efficient Numerical Model for Heat Transfer Simulation of Deep Borehole Heat Exchangers[J]. Energy and Buildings 2018;167:79-88.

[3] Holmberg, Henrik, José A, et al. Thermal Evaluation of Coaxial Deep Borehole Heat Exchangers[J]. Renewable Energy 2016;97:65-76.

[4]Le L, Morgan, François L, et al. Thermal Performance of a Deep Borehole Heat Exchanger: Insights from a Synthetic Coupled Heat and Flow Model[J]. Geothermics 2015:57:157-72.

[5] Liu J, Wang FH, Cai WL, et al. Numerical Study on the Effects of Design Parameters on the Heat Transfer Performance of Coaxial Deep Borehole Heat Exchanger[J]. International Journal of Energy Research 2019.

[6] Sapinska-Sliwa, Aneta, Marc AR, et al. Deep Borehole Heat Exchangers — a Conceptual and Comparative Review[J]. International Journal of Air-Conditioning and Refrigeration 2016;24:01.

[7] Sliwa T, Nowosiad T, Vytyaz O, et al. Study on the Efficiency of Deep Borehole Heat Exchangers[J]. SOCAR Proceedings 2016;2:29-42.

[8] Wang GS, Song XZ, Shi Y, et al. Numerical Investigation on Heat Extraction Performance of an Open Loop Geothermal System in a Single Well[J]. Geothermics 2019;80:170-84.

[9] Wang ZH, Wang FH, Liu J, et al. Field Test and Numerical Investigation on the Heat Transfer Characteristics and Optimal Design of the Heat Exchangers of a Deep Borehole Ground Source Heat Pump System[J]. Energy Conversion and Management 2017;153:603-15.

[10] Welsch, Bastian, Wolfram R, Daniel O. et al. Characteristics of Medium Deep Borehole Thermal Energy Storage[J]. International Journal of Energy Research 40 2016;13:1855-68.

[11] Kong YL, Chen CF, Shao HB, et al. Principle and Cpacity Qantification of Deep-norehole Heat Exchangers[J]. Geophys 2017;12:4741-52.